International Journal of Engineering Research and Technology. ISSN 0974-3154, Volume 13, Number 12 (2020), pp. 5283-5292

Sensorless Field-Oriented Control of Doubly-Fed Induction Motor Drive

Maxim Bobrov

Ogarev Mordovia State University, Dept. of Elect. & Electrical Engineering, Saransk, 430005, Russia

Abstract

In this article the electric drive based on the doubly-fed induction motor drive field-oriented control system without a flux-linkage and speed sensor is presented. Functional schemes are considered, model of speed observer and two models of flux-linkage observers are presented – observer by using the rotor voltage value and observer with current model. The stability margin of the field-oriented control system with observers models is determined by the D-decomposition method. The influence of the approximation accuracy of doubly-fed induction motor magnetization curve on the flux-linkage estimation by a current model of observer is investigated. The results of theoretical and experimental research are confirmed.

Keywords: Electric drive, Flux-linkage observer, Simulation, Speed observer, Stability

I. INTRODUCTION

The development of microcontroller control systems has created new op-portunities in power electronics and electric power industry. Currently, most con-trol systems in power electronics are implemented using microprocessors. This has served as a steady trend for replacing hardware solutions with software in various automated control systems. Also, in AC adjustable speed electric drive systems, sensors are replaced by state observers. The reduction in the number of mechanical components of the adjustable electric drive and the implementation of speed and flux-linkage observers leads to an increase in the reliability of the sys-tem. The issues of research and implementation of the AC drives speed and flux-linkage observers in a large number of Russian and foreign scientific papers and articles are presented [12; 25; 11; 10; 1; 5; 24; 4; 15; 3].

I.I Problem Definition and Research Goals

In most cases in flux vector control systems is necessary to estimate two variables: flux-linkage, in order to orient the vector system by its vector and speed or electromagnetic torque, in order to control it [15].

In a number of industrial areas in high-power electric drive systems, a dou-bly-fed motor is widely used. In the electric drive based on the doubly inverter-fed induction motor with two power converters in rotor and stator circuits (Fig.1) which is one of the option of double-fed induction machine there is a possibility to measure the frequencies of currents and voltages in the rotor and the stator cir-cuits. It makes possible to offer a simple algorithm of speed estimation and im-plement the speed observer which is robust to the change of the motor parame-ters [19; 14; 6; 20; 22; 2].

But at the energy-efficient control algorithms implementing which provide the high energy efficiency to drive, information about motor magnetic state is needed [23; 16; 18].

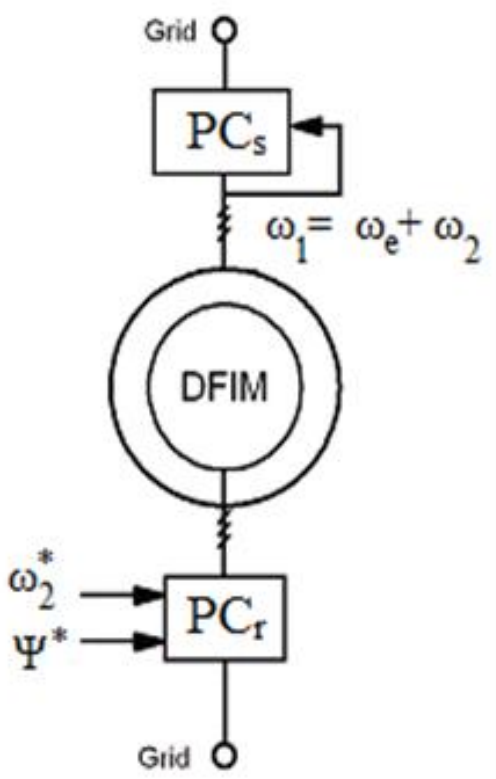

Figure 1. Electric drive based on double inverter-fed induction motor struc-tural scheme

The analysis of the electric drive model taking into account the generally accepted assumptions [7; 8; 13] is carried out. It is most expedient to choose the x, y orthogonal coordinate system oriented along the vector of flux-linkage in the air gap Ψ_δ [21].

II. THEORY AND SIMULATION

The functional schemes of flux observers for electric drive based on double inverter-fed induction motor [14]. The rotor and stator equations system in x, y coordinate system:

$$\begin{cases} U_{sx} = R_s i_{sx} + \dfrac{d\psi_{sx}}{dt} - \omega_1 \psi_{sy}; \\ U_{sy} = R_s i_{sy} + \dfrac{d\psi_{sy}}{dt} + \omega_1 \psi_{sx}; \\ U_{rx} = R_r i_{rx} + \dfrac{d\psi_{rx}}{dt} - \omega_2 \psi_{ry}; \\ U_{ry} = R_r i_{ry} + \dfrac{d\psi_{ry}}{dt} + \omega_2 \psi_{rx}, \end{cases} \quad (1)$$

Where

$$\begin{cases} \psi_{sx} = L_{ls} i_{sx} + \psi_{\delta x}; \\ \psi_{sy} = L_{ls} i_{sy} + \psi_{\delta y}; \\ \psi_{rx} = L_{lr} i_{rx} + \psi_{\delta x}; \\ \psi_{ry} = L_{lr} i_{ry} + \psi_{\delta y}. \end{cases} \quad (2)$$

To synthesize of the flux observer by using the values of rotor voltage the pairs of the last equations from systems (1) and (2) respectively are used, substi-tuting the value of the rotor flux projections into the equations of rotor voltages:

$$\begin{cases} U_{rx} = R_r i_{rx} + L_{lr} \dfrac{di_{rx}}{dt} + \dfrac{d\psi_{\delta x}}{dt} - \omega_2 \psi_{\delta y} - \omega_2 L_{lr} i_{ry}; \\ U_{ry} = R_r i_{ry} + L_{lr} \dfrac{di_{ry}}{dt} + \dfrac{d\psi_{\delta y}}{dt} + \omega_2 \psi_{\delta x} + \omega_2 L_{lr} i_{rx}. \end{cases} \quad (3)$$

Represents it in Cauchy form. Flux through the remaining variables of the equations is expressed:

$$\begin{cases} \dfrac{d\psi_{\delta x}}{dt} = U_{rx} - R_r i_{rx} - L_{lr} \dfrac{di_{rx}}{dt} + \omega_2 L_{lr} i_{ry} + \omega_2 \psi_{\delta y}; \\ \dfrac{d\psi_{\delta y}}{dt} = U_{ry} - R_r i_{ry} - L_{lr} \dfrac{di_{ry}}{dt} - \omega_2 L_{lr} i_{rx} - \omega_2 \psi_{\delta x}. \end{cases} \quad (4)$$

Replacing $\dfrac{d}{dt} = p$ and $T_{lr} = \dfrac{L_{lr}}{R_r}$, obtain equations for the projections of the air gap flux in the *x, y* coordinate system:

$$\begin{cases} \psi_{\delta x} = \dfrac{U_{rx}}{p} - (1 + T_{lr} p)\dfrac{i_{rx} R_r}{p} + \dfrac{\omega_2 L_{lr} i_{ry}}{p} + \dfrac{\omega_2 \psi_{\delta y}}{p}; \\ \psi_{\delta y} = \dfrac{U_{ry}}{p} - (1 + T_{lr} p)\dfrac{i_{ry} R_r}{p} - \dfrac{\omega_2 L_{lr} i_{rx}}{p} - \dfrac{\omega_2 \psi_{\delta x}}{p}. \end{cases} \quad (5)$$

Taking into account that the *x, y* coordinate system is oriented along the air gap flux vector $|\dot{\Psi}_\delta| = \Psi_{\delta x}$ and $\Psi_{\delta y} = 0$, the transfer function of the flux observer can be defined as:

$$W_\Psi(p) = \frac{\psi_{\delta x}}{(\omega_2 L_{lr} i_{ry} + U_{rx})\dfrac{1}{1 + T_{lr} p} - i_{rx} R_r} = \frac{1 + T_{lr} p}{p}. \quad (6)$$

The functional scheme of an electric drive model is based on double inverter-fed induction motor with a flux observer by using the rotor voltage.

The implementation of the electric drive based on the double inverter-fed induction motor with two power converters in rotor and stator circuits with a magnetic flux observer by using the rotor voltage simulation model in Matlab-Simulink software is shown in Fig. 2. In the simulation model the parameters of an induction motor with wound rotor of the industrial series 4AK250SB4U3 with a rated power 55 kW are used.

After the synthesis of sensorless vector control system it is expedient to check the convergence of the results obtained with the using of two simulation models working in parallel - sensorless (Fig.2) and a model with block which simulate a flux sensor [6]. As the base machine in both models the motor with wound rotor 4AK250SB4U3 is chosen. The results of transient simulation (from top to bottom) of magnetic flux, electromagnetic torque, stator current and speed during acceleration of the motor and change of the torque to nominal values are shown in Fig. 3.

Up to a time period of 0.2 seconds the motor is magnetized along the rotor circuit at zero speed. This period is sufficient for the magnetic flux of the motor to reach the rated value. Then a signal to the power converter control system in stator circuit for producing the electromagnetic torque and speed is fed. The load on the shaft is 60% of the rated value. At the initial moment a small dip in the speed curve is observed, which is caused by the saturation of the inertial links of the model (wind-up effect). After 0.7 seconds of simulation, the load is increased to rated value.

The obtained results indicate complete convergence of the transient processes in the simulated of drive systems - in simulation model with block which imitate measurement of flux by Hall sensors and in model with synthesized observer using the rated value of the rotor resistance R_r' in the model of observer.

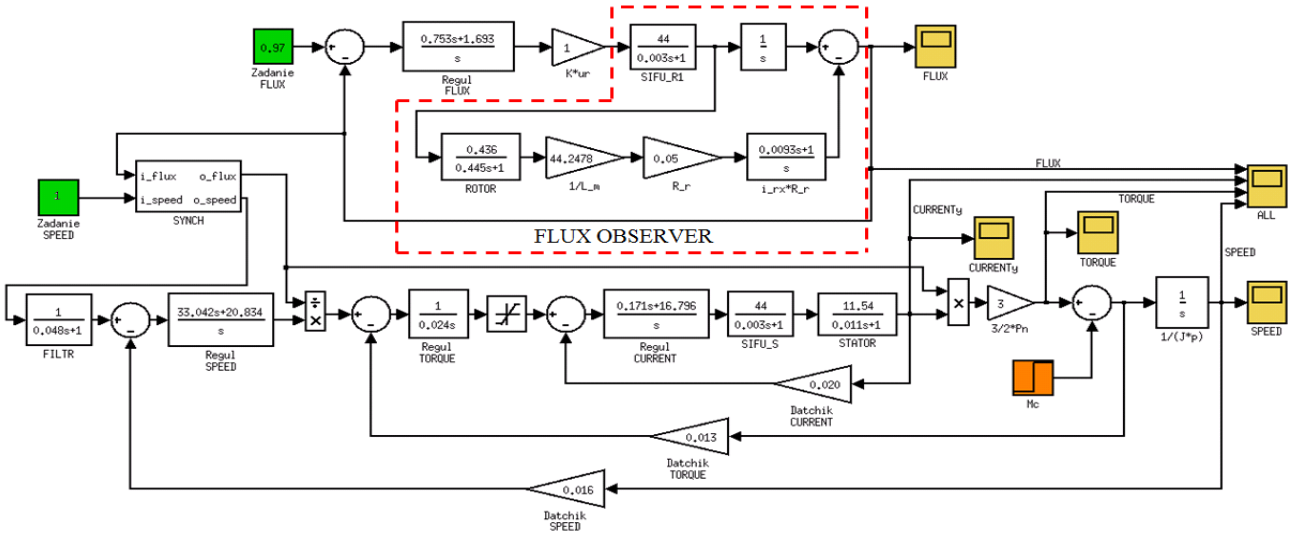

Figure 2. Electric drive based on the double inverter-fed induction motor with two power converters in rotor and stator circuits with flux observer by using the ro-tor voltage simulation model in Matlab-Simulink software

The structure of the observer model isn't included mutual inductance, i.e. the nonlinearity of the magnetization curve at the implementation of energy-efficient control with a variable flux will not lead to an error in the estimation of the flux value. However, the value of the rotor resistance which is included in ob-server model in different operation modes can vary significantly compared to the rated value [11; 7; 20; 22; 9; 17]. To evaluate the robustness of the synthesized observer it is necessary to find the stability area of the system with respect to the parameter R_r' by the *D*-decomposition method.

The characteristic equation of transfer function of flux control loop looks:

$$H = T_{pn}p^2(T_n p+1)(T_r p+1) + k_{on}k_n k_{pn}(T_{pn}p+1)(T_r p - R_r R_r' T_{lr} p - R_r R_r' + 1). \quad (7)$$

After the transformations and the introduction of a new variable $k_{on}k_n k_{pn} = a$, the characteristic equation takes the form:

$$H = T_{pn}T_n T_r p^4 + T_{pn}T_n p^3 + T_r T_{pn} p^3 + T_{pn}p^2 + aT_r T_{pn}p^2 - a\left(T_{lr}T_{pn}R_r R_r' p^2 + T_{pn}p + T_r p - T_{pn}R_r R_r' p - T_{lr}R_r R_r' p - R_r R_r' + 1\right). \quad (8)$$

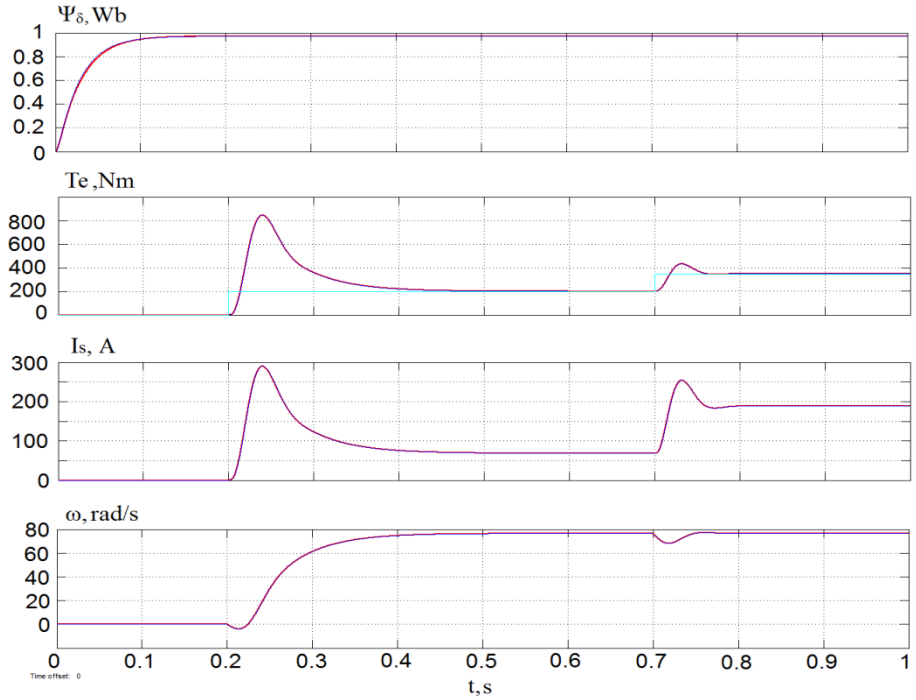

Figure 3. Simulation results of the (from top to bottom) flux, electromagnetic torque, stator current and speed transient

Expressing the rotor resistance from the characteristic equation obtained the following relation:

$$R_r^{'} = \frac{T_{pn}T_nT_rp^4 + T_{pn}T_np^3 + T_rT_{pn}p^3 + T_{pn}p^2 + a\left(T_rT_{pn}p^2 + T_{pn}p + T_rp + 1\right)}{-a\left(T_{lr}T_{pn}R_rp^2 - T_{pn}R_rp - T_{lr}R_rp - R_r\right)}. \quad (9)$$

The coefficient *a* and the time constants of the control loops are known numerical values. Therefore, the and substituting numerical values of the time constants and coefficients of the electric drive model based on the 4AK250SB4U3 motor it can be written in the following form:

$$R_r^{'} = \frac{0.000787_r\,p^4 + 0.2644_n\,p^3 + 9.293p^2 + 34.3p + 33.14}{0.009437\,p^2 - 1.03p + 1.7199}. \quad (10)$$

To create the locus of the system LabVIEW software is applied (Fig.4, Fig.5).

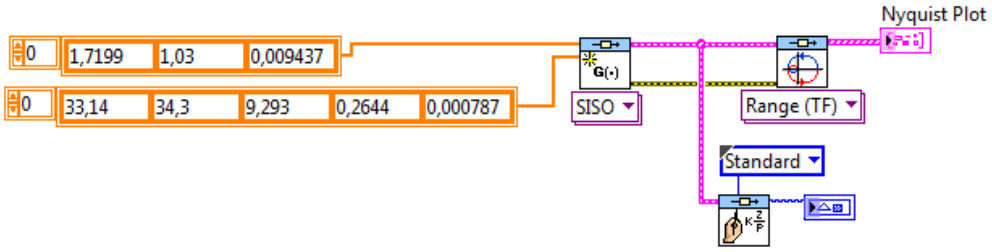

Figure 4. Program in Labview software for locus creation

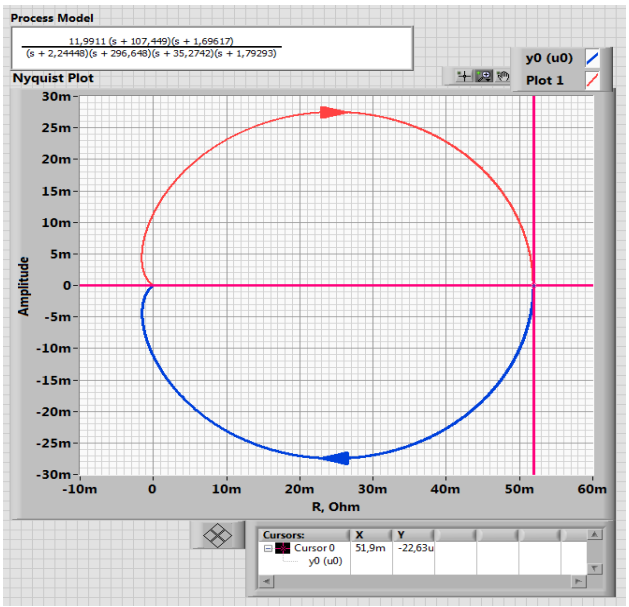

Figure 5. Locus in Labview software

The locus has a classical shape for the inertial link and crosses the X-axis at the point with coordinates (0.00519; 0). In that the values of the parameter R_r' are real and always positive the most interesting is the positive real semi-axis of the locus.

At the solving of the characteristic equation with a parameter R_r' all its roots are smaller than locus margin so that area inside the locus is indeed an area of stability. Substitution of the values of the rotor resistance into the characteristic equation is larger than the margin value leads to the appearance roots which are larger than locus margin. The results of transient simulation in Matlab-simulink (from top to bottom) of magnetic flux, electromagnetic torque, stator current and speed during acceleration of the motor with $R_r' = 1.15R_r'$ which is R_r' on 15% larger than the margin value are shown in Fig. 6.

It is obvious that if the parameter exceeds the margin values, the observed value of the magnetic flux at the saturation section of the magnetization curve deviates significantly from the value

obtained in the simulation of the system using magnetic flux sensors and the system becomes unstable [26].

Thus, the observer is sensitive to a change in resistance and if it deviates by 5-10% of the rated value system becomes unstable.

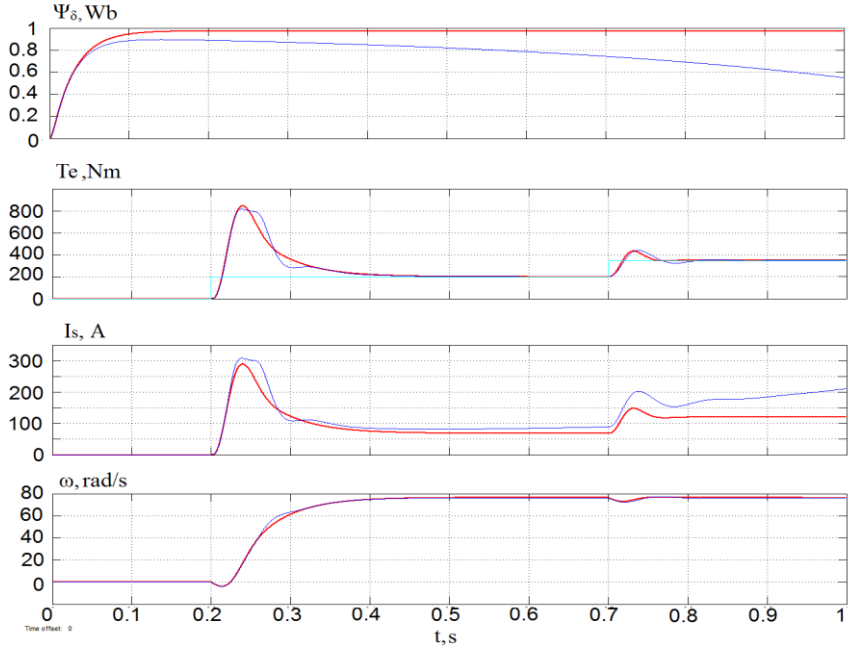

Figure 6. Simulation results of the (from top to bottom) flux, electromagnetic torque, stator current and speed transient with $R'_r = 1.15R'_r$

In order to solve this problem the methods used in other types of AC drives are valid in the DIFIM drive:

- To reduce the error in estimation the value of the rotor resistance in the observer model should be set equal to the rotor resistance in the heated state [11];
- Parametric adaptation to the changing parameters of the base machine [15; 3].

However, these approaches have drawbacks - it is difficult to accurately determine the parameters of the machine, and the implementation of adaptive algorithms requires a significant consumption of processor resources.

In addition, the rotor voltage has a DC component the integration of which leads to an accumulation of error at the integrator output and as a consequence incorrect estimation of the flux. To correct the operation mode of the integrator and eliminate the influence of the DC component it is necessary to introduce a weak negative feedback into the integrator.

Taking into account the indicated drawbacks of the flux-linkage observer with voltage model, let's consider current model of the magnetic flux observer. The scalar form of writing equations (1) in a coordinate system oriented along the air gap magnetic flux vector ($\Psi_{\delta y} = 0$) will take the form:

$$\begin{cases} L_{ls}\dfrac{di_{sx}}{dt} = U_{sx} - R_s i_{sx} - \dfrac{d\Psi_{\delta x}}{dt} + \omega_1 L_{ls} i_{sy}, \\ L_{ls}\dfrac{di_{sy}}{dt} = U_{sy} - R_s i_{sy} - \omega_1 L_{ls} i_{sx} - \omega_1 \Psi_{\delta x}, \\ \dfrac{d\Psi_{\delta x}}{dt} = -\dfrac{R_r}{L_r}\Psi_{\delta x} + \dfrac{L_m}{L_r}R_r i_{sx} + L_{lr}\dfrac{L_m}{L_r}\dfrac{di_{sx}}{dt} - \omega_2 L_{lr}\dfrac{L_m}{L_r}i_{sy} + \dfrac{L_m}{L_r}U_{rx}, \\ 0 = \dfrac{L_m}{L_r}R_r i_{sy} + L_{lr}\dfrac{L_m}{L_r}\dfrac{di_{sy}}{dt} - \omega_2 \Psi_{\delta x} + \omega_2 L_{lr}\dfrac{L_m}{L_r}i_{sx} + \dfrac{L_m}{L_r}U_{ry}. \end{cases} \quad (11)$$

From the third equation of the system determine the transfer function of the flux observer.

In an electric drive based on double inverter-fed induction motor the base motor is magnetized along the rotor circuit ($i_{sx} = 0$), and the EMF $\omega_2 L_{lr}\dfrac{L_m}{L_r}i_{sy}$ is compensated in the control system compensation block, therefore, the final transfer function will look like:

$$W_{\Psi_{\delta\_1}}(p) = L'_m i_{rx}\frac{1}{T_r p + 1}. \quad (12)$$

In this model of the flux observer there is a parameter of mutual inductance, which varies depending on the operating mode of the motor.

The results of the simulation show an error of at least 15% in the estimation of the magnetic flux in the low-load region with

a change of 50% of the nominal value, which affects to the dynamics (Fig. 7) and losses in the magnetizing circuit [23]. But in general, the system remains stable when a magnetic flux is reached.

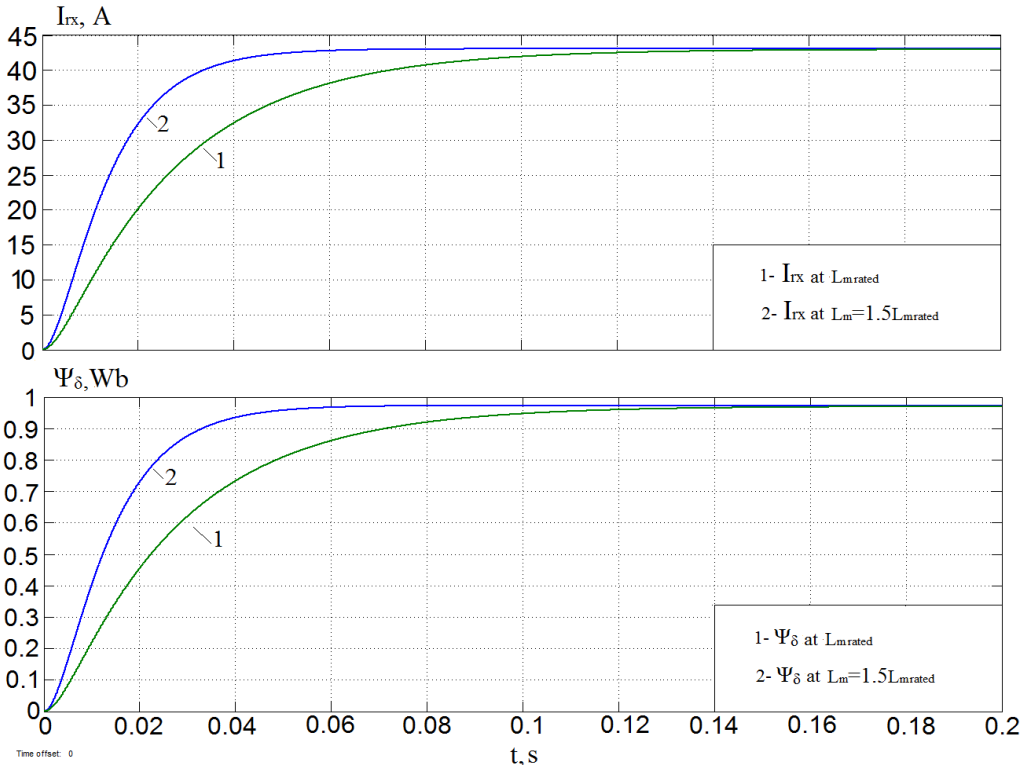

Figure 7. Simulation results of magnetic flux and currents comparison with L_m=1.5 L_m

In Fig. 8 represents the simulation model of two drive systems - with mod-els of observers and with the Machines Measurement Demux block as the flux sensor. In the latter, the motor parameters are equal to their nominal values, and in the sensorless it is changed within the limits considered above. The results of simulation of magnetic fluxes are shown in Figure 9.

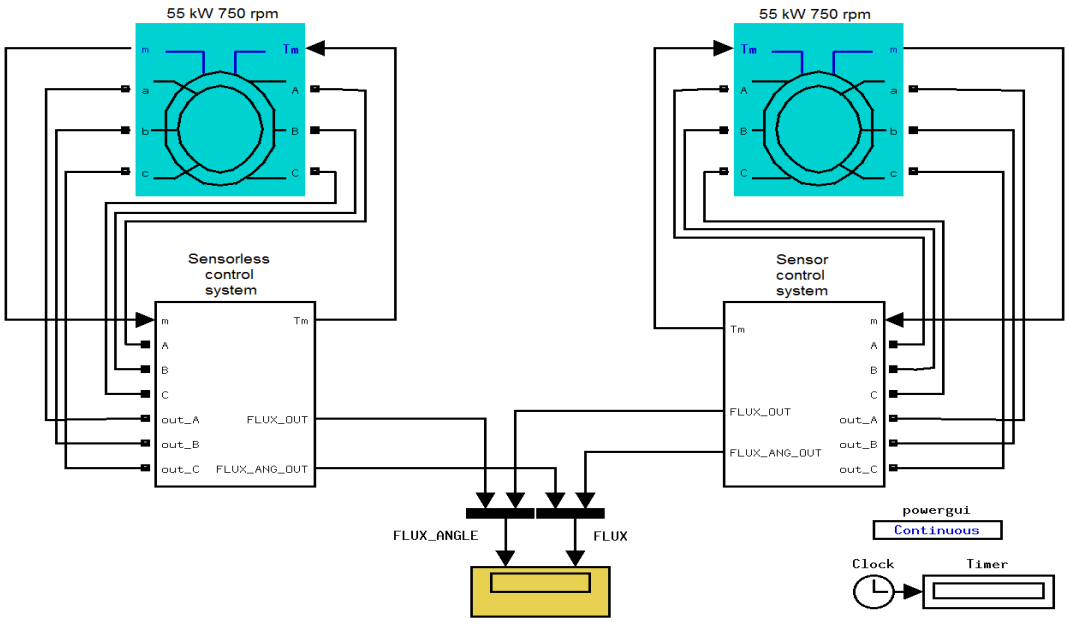

Figure 9 a) Simulation results of flux with $R_r' = 1.15R_r'$, b) Simulation results of flux with L_m=1.5 L_m

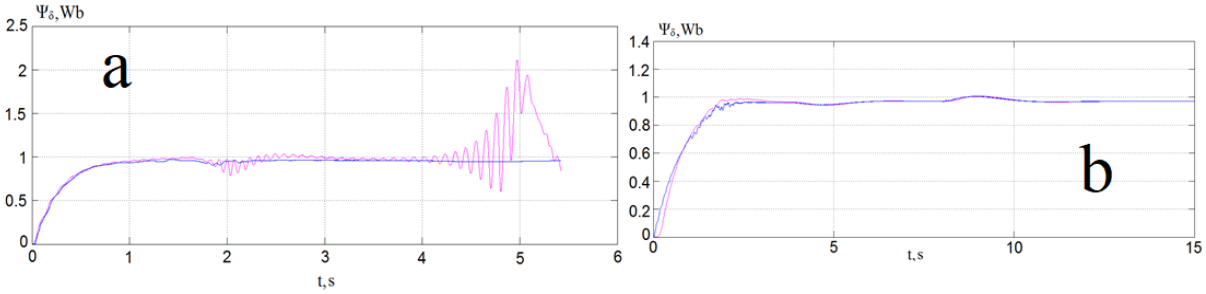

Figure 8. Simulation model of two drive systems

In this option of electric drive, a speed observer model is implemented easier than with an induction or permanent magnet synchronous motor electric drive.

III. EXPERIMENTAL RESULTS

For experimental verification the experimental setup was developed. DFIM electric drive functional scheme is shown at Fig.10. Current and voltage sensors in the rotor circuit and current sensors in the stator circuit determine the instantaneous values of rotor currents and voltages, as well as stator current, which are further used as signals for constructing coordinate observers. The blocks of coordinate transformations are implemented according to the equations of the mathematical model [19; 2] are integrated into the block of the machine flux-linkage observers. This block contains models of two flux-linkage observers, which are switched due to the logical switch by the feedback signal of the magnetization current i_{rx}.

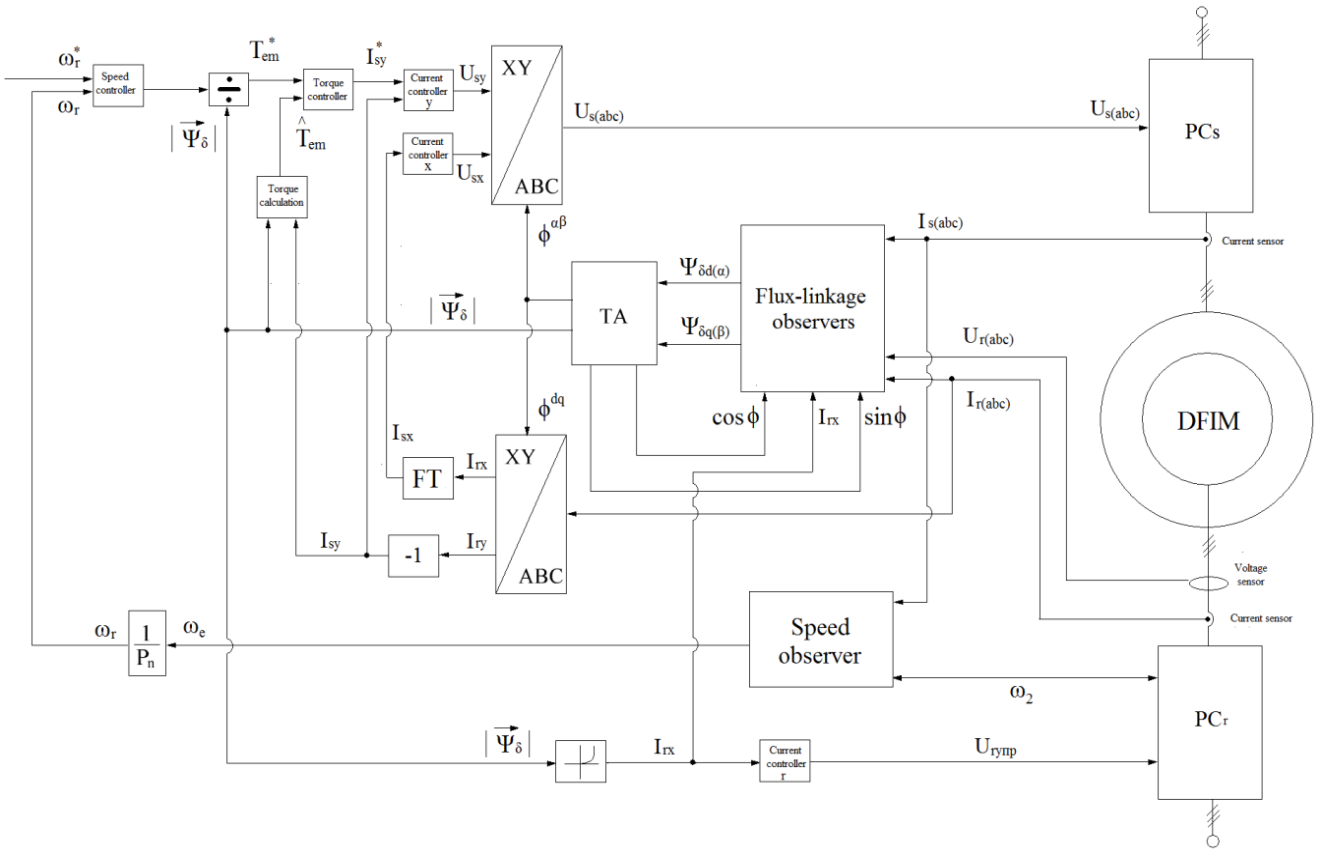

Figure 10. DFIM electric drive functional scheme

The experimental setup consists of DFIM, two power converters in stator and rotor circuits, DC motor in load operation mode, encoder on the shaft, measure-ment equipment and PC with Matlab and LabView software.

The results of the estimated and experimental flux-linkage value by two models of observers are shown in Fig. 11. For current model of flux-linkage observer at the linear section of the magnetization curve the error between the estimated data and the obtained ones was experimentally $\Delta\Psi_{\pi uH}$ = 13.6%, and for the saturation section - $\Delta\Psi_{\pi uH}$ = 4.81%.

For voltage model of flux-linkage observer at the linear section of the magnetization curve the error between the estimated data and the obtained ones was experimentally $\Delta\Psi_{\pi uH}$ = 9.4%, and for the saturation section - $\Delta\Psi_{\pi uH}$ = 14.89%.

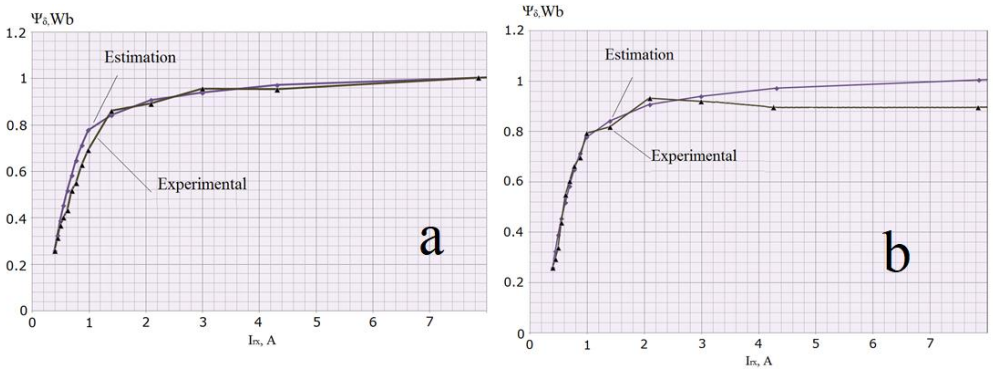

Figure 11. a) Dependences of Ψδ=f (Im) for flux-linkage observer using current value for estimation, b) Dependences of Ψδ=f (Im) for flux-linkage observer using voltage value for estimation

Speed estimation strategy does not contain in the algorithm of the rotor speed estimation trigonometric functions, parameters of the base machine, does not depend on the operating mode of the ED, allow estimating the speed of the rotor with an error of no more than 5% at a rotor speed of 10-30% of the nomi-nal values (Fig.12).

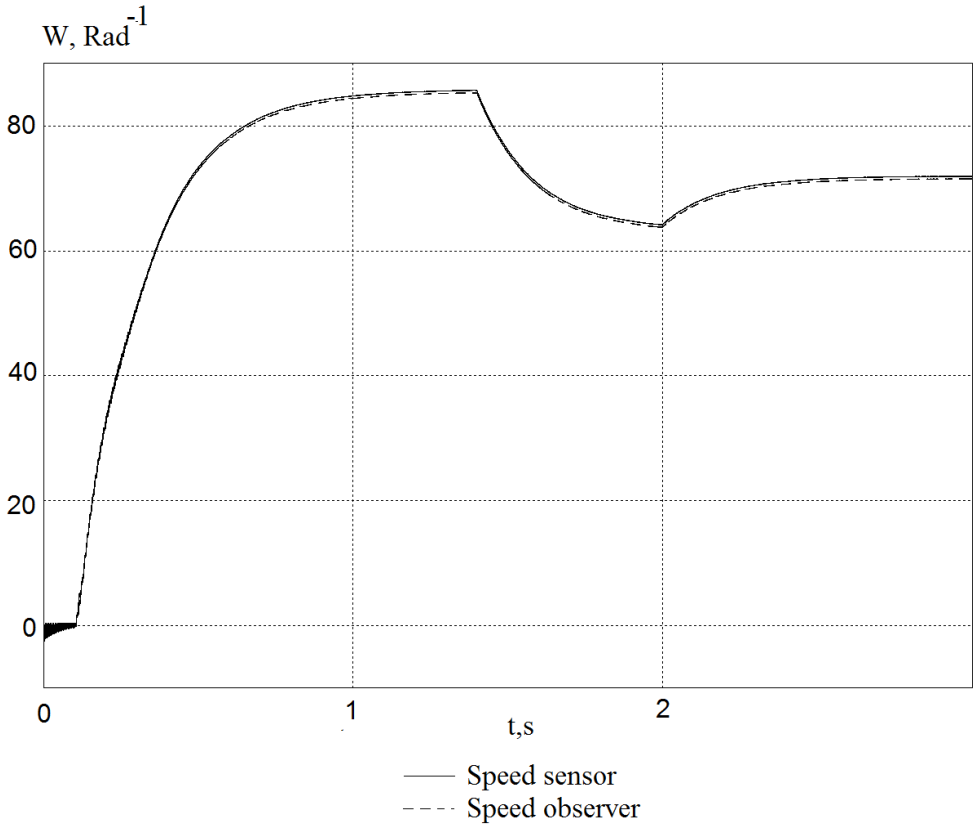

Figure 12. Dependences of ω=f (t) at Tem = Temrated and changing ω

In this electric drive system identification of flux-linkage at zero angular ve-locity of the rotor is possible. This is laid down in the principle of the operation of a DFIM, controlled by two circuits, when the magnetization of the machine is carried out before the stator PC is turned on. In this case, and flux-linkage is pro-duced only by the excitation current in rotor circuits.

IV. CONCLUSION

The proposed algorithms for estimation of air gap magnetic flux-linkage make it possible to exclude a flux sensor from the control system of the electric drive and use a serial motor with a wound rotor as the base machine. The ob-server for the voltage of the rotor is sensitive to the change in resistance and if it deviates by 5-10% of the nominal value causes the FOC system is become unsta-ble.

Great influence on the evaluation of flux is due to the presence of a DC component in the rotor voltage. To compensate for the integration error, it is nec-essary to introduce feedback into the integrator structure.

The application of the current model leads to errors of at least 15% in the estimation of the magnetic flux in the low-load region, which affects the dynamics and losses in the magnetizing circuit. But in general, the system remains stable when a specified magnetic flux is reached. Both proposed models of observers allow estimating the value of the flux when the rotor is stationary.

REFERENCES

[1] Afanas'ev KS, Glazyrin AS. Speed identification of experimental setup induc-tion motor Афанасьев using Kalman filter and Luenberger observer. Electrical engineering complexes and systems. 2012;4:66-69.

[2] Amar A, Belkacem SB, Mahni T. Direct torque control of a doubly fed induction generator. International Journal of Energetica. 2017;2(1):11-14,.

[3] Ananth DVN, Kumar GV. Tip Speed Ratio Based MPPT Algorithm and Improved Field Oriented Control for Extracting Optimal Real Power and Independent Reactive Power Control for Grid Connected Doubly Fed Induction Generator. International Journal of Electrical & Computer Engineering. 2016;6(3):2088-8708.

[4] Bobrov MA, Tutaev GM. Estimation of the energy characteristics of DIFIM for different methods of approximating the magnetization curve. Russian electrical engineering. 2017;6:2-6.

[5] Deoliveira DD, Vieira RP, Gründling HA. A quasi-sliding mode speed and position observer with a chattering elimination filter. IEEE 13th Brazilian Power Electronics Conference and 1st Southern Power Electronics Con-ference (COBEP/SPEC). 2015;1:1-6.

[6] Díaz SA, Silva CA, Juliet J, Delpino HM. Novel anti-windup scheme for stator flux control in surface permanent magnet machines. In 2017 IEEE Texas Power and Energy Conference (TPEC). 2017:1-6. IEEE.

[7] Elmahfoud M, Bossoufi B, Taoussi M, El Ouanjli N, Derouich A. Rotor Field Oriented Control of Doubly Fed Induction Motor. In 2019 5th International Conference on Optimization and Applications (ICOA). 2019:1-6. IEEE.

[8] Fayssal A, Chaiba A, Babas B, Mekhilef S. Design and implementation of high performance field oriented control for grid-connected doubly fed induction generator via hysteresis rotor current controller. Rev. Roum. Sci. Techn.-Electrotechn. Et Energ. 2016;61(4):319-324.

[9] Fayssal A, Chaiba A, Francois B, Babes B. Experimental design of stand-alone field oriented control for WECS in variable speed DFIG-based on hysteresis current controller. In 2017 15th International Conference on Electrical Machines, Drives and Power Systems (ELMA).2017;304-308. IEEE,.

[10] Mengoni M, Zarri L, Tani A, Serra G, Casadei D. Sensorless speed observer based on third-order spatial field harmonic for multiphase induction motor drives. IEEE Symposium on Sensorless Control for Electrical Drives (SLED). 2016;5(1):1-6.

[11] Mesheryakov VN, Bezdeneznykh DV. Flux linkage observer for DFIM, controlled at stator and rotor circuits. Bulletin of Voronezh STU. 2010;6(11):170-173.

[12] Mohamadian S. A novel flux observer and switching scheme for LCI-fed synchronous motor drives. 8th Power Electronics, Drive Systems & Technologies Conference (PEDSTC). 2017;1:425-430.

[13] Najib E, Derouich A, El-Ghzizal A, Chebabhi A, Taoussi M. A comparative study between FOC and DTC control of the Doubly Fed Induction Motor (DFIM). In 2017 International Conference on Electrical and Information Technologies (ICEIT). 2017:1-6. IEEE.

[14] Othmane Z, El-Mourabit Y, Errouha M, Derouich A, El-Ghzizal A. Power control of variable speed wind turbine based on doubly fed induction generator using indirect field-oriented control with fuzzy logic controllers for performance optimization. Energy Science & Engineering. 2018;6(5):408-423.

[15] Rajeshkumar P, Mulla MA. A Novel Position-Sensorless Algorithm for Field-Oriented Control of DFIG With Reduced Current Sensors. IEEE Transactions on Sustainable Energy. 2018;10(3):1098-1108.

[16] Rajeshkumar P, Mulla MA. Mathematical Modeling and Position-Sensorless Algorithm for Stator-Side Field-Oriented Control of Rotor-tied DFIG in Rotor Flux Reference Frame. IEEE Transactions on Energy Conversion. 2019;1:1-7.

[17] Samir M, Hallouz M, Kabache N, Kouadria S. Neural Network Based Field Oriented Control for Doubly-Fed Induction Generator. International Journal of Smart Grid-ijSmartGrid. 2018;2(3):183-187.

[18] Tholath JJ, Chattopadhyay AB. Mathematical Formulation of Feedback Linearizing Control of Doubly Fed Induction Generator Including Magnetic Saturation Effects. Mathematical Problems in Engineering. 2020;1:1-11.

[19] Tutaev G, Bobrov M. Rotor speed estimation in control system of electric drive based on induction inverter-fed motor. IX International Conference on Power Drives Systems (ICPDS). 2016;1:1-4.

[20] Tutaev GM. Energy-efficient control options of electric drive based on asyn-chronous converter-fed motor', Proceedings of the 2016 13th International Scientific-Technical Conference on Actual Problems of Electronics Instrument Engineering (APEIE). 2016:88-93.

[21] Tutaev GM. Double inverter-fed induction motor energy performances research at analytical model. 2017 International Siberian Conference on Control and Communications, SIBCON - Proceedings 7998483. 2017.

[22] Tutaev GM. Development and research of flux linkage observers for sensorless control of double-fed induction motor drive. Journal of Advanced Research in Dynamical and Control Systems. 2018;10(4):1440 – 1447.

[23] Tutaev GM. Sensorless speed estimation in electric drive based on double in-verter-fed induction motor. Journal of Advanced Research in Dynamical and Control Systems. 2018;10(4):1448 – 1455.

[24] Udai S, Strous TD, Polinder H, Ferreira JA, Veltman A. Achieving sensorless control for the brushless doubly fed induction machine. IEEE Transactions on Energy Conversion. 2017;32(4):1611-1619.

[25] Alexsandrovna Galikhanova U, Arnoldovna Timofeeva O. Stevioside-induced molecular heterogeneity and lectin activity at low positive temperatures. Caspian Journal of Environmental Sciences. 2020 Dec 1;18(5):473-80.

[26]Xin Z, Zhao R, Blaabjerg F, Zhang L, Loh PC. An Improved Flux Observer for Field-Oriented Control of Induction Motors Based on Dual Second-Order Generalized Integrator Frequency-Locked Loop. IEEE Journal of Emerging and Selected Topics in Power Electronics. 2017;5(1):513-525.

BIOGRAPHIES OF AUTHOR

Maxim Bobrov is PhD in Technical Sciences. Head teacher of electronic & electrical engeneering department. Author of more then 50 papers and articles. Research interests: power electronic, adjustable speed AC electric drives, control theory and systems.